Materials Letters 274 (2020) 127968

Contents lists available at ScienceDirect

Materials Letters

journal homepage: www.elsevier.com/locate/mlblue

Process-microstructural features for tailoring fatigue strength of wire arc additive manufactured functionally graded material of SS904L and Hastelloy C-276

A. Rajesh Kannan [a], S. Mohan Kumar [a], N. Pravin Kumar [a], N. Siva Shanmugam [a,*], A.S. Vishnu [b], Yasam Palguna [c]

[a] Department of Mechanical Engineering, National Institute of Technology, Tiruchirappalli, Tamil Nadu, India
[b] Department of Mechanical Engineering, National Institute of Technology, Surathkal, Karnataka, India
[c] Department of Materials Science and Metallurgical Engineering, Indian Institute of Technology, Hyderabad, Telangana, India

ARTICLE INFO

Article history:
Received 23 April 2020
Received in revised form 5 May 2020
Accepted 10 May 2020
Available online 16 May 2020

Keywords:
Fatigue
Welding
Microstructure
WAAM
Mechanical properties

ABSTRACT

Many engineered components on subjecting to critical environments require properties that slightly differs with location in the fabricated part. The inadequate understanding of wire arc additive manufacturing (WAAM) process-microstructural features correlation brings interests on the structural reliability of functionally graded materials (FGM), which limits the extensive use of this cutting edge technology. Gas metal arc welding (GMAW) based WAAM process was adopted to fabricate the FGM of super austenitic stainless steel SS904L and Hastelloy C-276 with excellent bonding. The micrographs revealed that the WAAM processed FGM was mainly composed of columnar and equiaxed dendrites and had noticeable inhomogeneous features along the built direction. Tensile test results of sample along the built direction revealed a yield strength of 311.08 MPa and tensile strength of 680.73 MPa. Cyclic loading results depicted that the WAAM processed FGM has a fatigue resistance of 156 Mpa after sustaining 2×10^6 cycles. As a result of the varying microstructural characteristics along the built direction, the failure was initiated and fractured at the SS904L weaker region.

1. Introduction

Additive Manufacturing (AM) techniques are of great interest because of their revolutionary role in various industries such as automotive, aviation, medicine, etc. [1]. However, the main challenge with AM is obtaining excellent mechanical properties from the structure without any defects such as macro voids, pores, high surface roughness and anisotropic microstructure [2]. WAAM process is highly efficient and economical approach for the fabrication of large structures in the open working environments [3]. WAAM has been extensively used to deposit multipart designed structures, however less interest has been put into developing functionally graded materials (FGM). FGM's are highly preferred in aviation industries, nuclear power stations and extreme conditions where varying properties are desired [4]. Among a few studies, Ramkumar et al [5] welded SS904L and Inconel 625 using ERNiCrMo-4 filler wire using Gas tungsten Arc Welding (GTAW) process and reported the microsegregation of Mo/Nb rich phases. Sharma et al [6] made an attempt to weld AISI 321 and Hastelloy C-276 using ERNiCrMo-4 filler wire via GTAW process and revealed that the tensile specimens fractured away from weld metal with tensile strength higher than AISI 321 base metal. SS904L is a non-stabilized steel with lower wt% of carbon and this alloy offers excellent weldability and forming properties. Hastelloy C276 is a Ni-Mo-Cr superalloy which has superior corrosion resistance over a wide range of severe environments. Hasan et al [7] fabricated FGM of low carbon steel and SS 316L using GMAW based WAAM process without any flaws and reported higher hardness at the interface as a result of the migration of Cr from SS316L. FGM of Ti–6Al–4 V/Al–6.25Cu was fabricated via cold metal transfer (CMT) WAAM process and observed brittle facture in the tensile samples [8]. In addition, it was noticed that depositing Ti alloy first was better for manufacturing Ti/Al structures without defects. Carneiro et al [9] compared the fatigue strength of 17–4 PH steel (300 MPa) fabricated by selective laser melting and conventionally manufactured 17–4 PH steel (640 MPa). It is evident from the available literature, FGM of SS904L/Hastelloy C-276 finds application in harsh environments such as oil and gas industries and nuclear power plants for fabricating steam generator, reformers,

* Corresponding author.
E-mail address: nsiva@nitt.edu (N. Siva Shanmugam).

https://doi.org/10.1016/j.matlet.2020.127968
0167-577X/

Table 1
Chemical composition of the filler wires ER904L and ERNiCrMo-4.

Filler wire	Element/wt %											
	Ni	Cr	Mo	Co	Mn	V	Cu	S	Fe	Si	W	C
ERNiCrMo-4	57.2	16.2	16.3	0.1	0.61	0.16	0.03	0.002	5.7	0.08	3.6	0.01
ER 904L	23.1	20.3	4.1	–	1.39	–	1.26	0.004	49.4	0.37	–	0.02

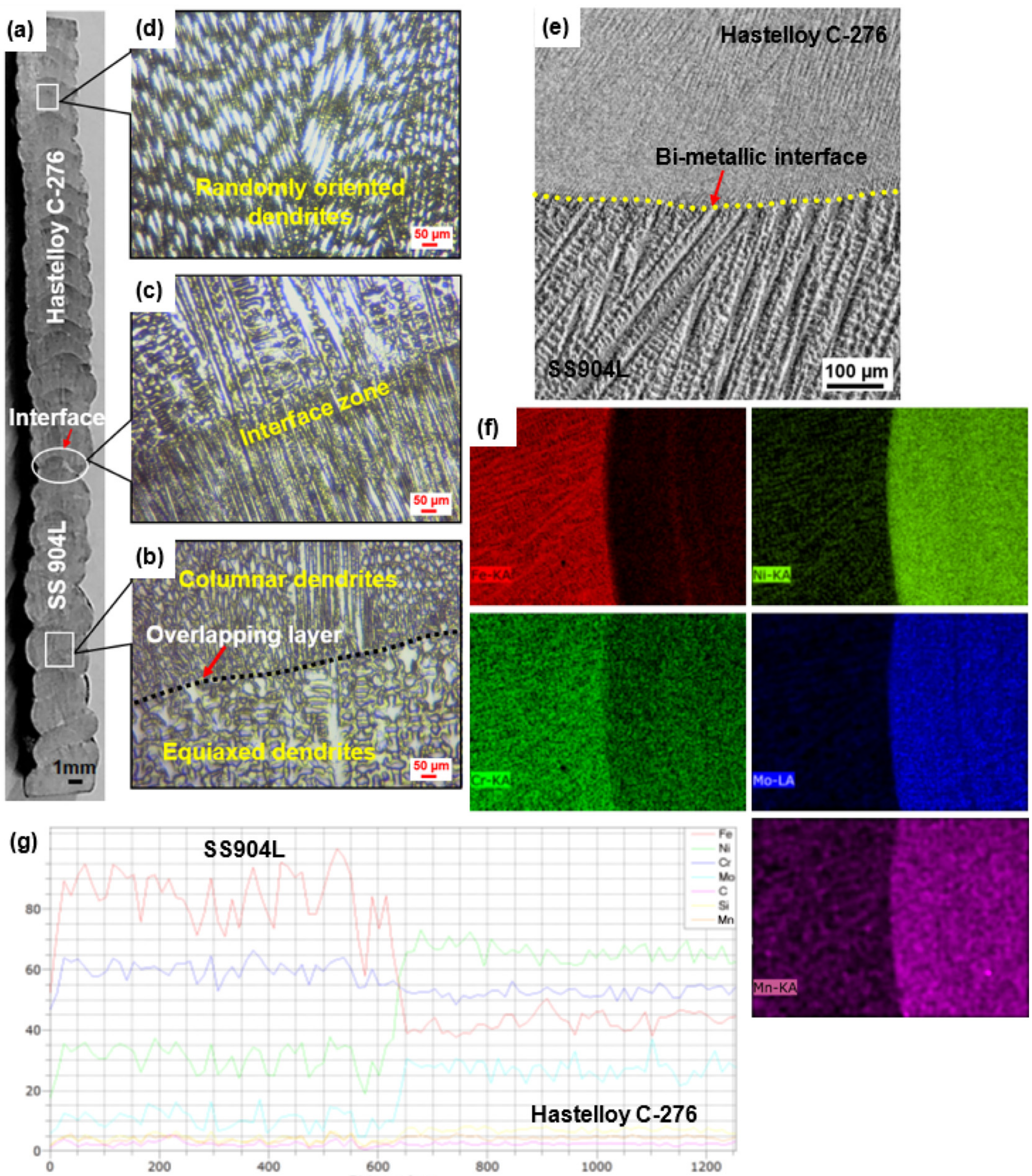

Fig. 1. Micro-chemistry of the WAAM processed FGM: (a) overall macrograph, (b–d) microstructures at various regions (e) SEM micrograph, (f) EDS elemental mapping and (g) EDS line scan at the bi-metallic interface.

etc [5–6]. Hence, FGM of SS904L/Hastelloy C-276 needs further consideration because of sparse literature. The aim of our research is to evaluate the influence of microstructure on tensile and fatigue behaviour of WAAM processed FGM. This research reports the true potential of WAAM process to fabricate FGMs for specific environments with desired properties.

2. Experimental details

The FGM was deposited in a layer-by-layer technique using GMAW based WAAM process. The filler wires used for deposition were SS904L and Hastelloy C-276 of 1.2 mm diameter. The substrate material was 904L plate. The chemical composition of the filler wires

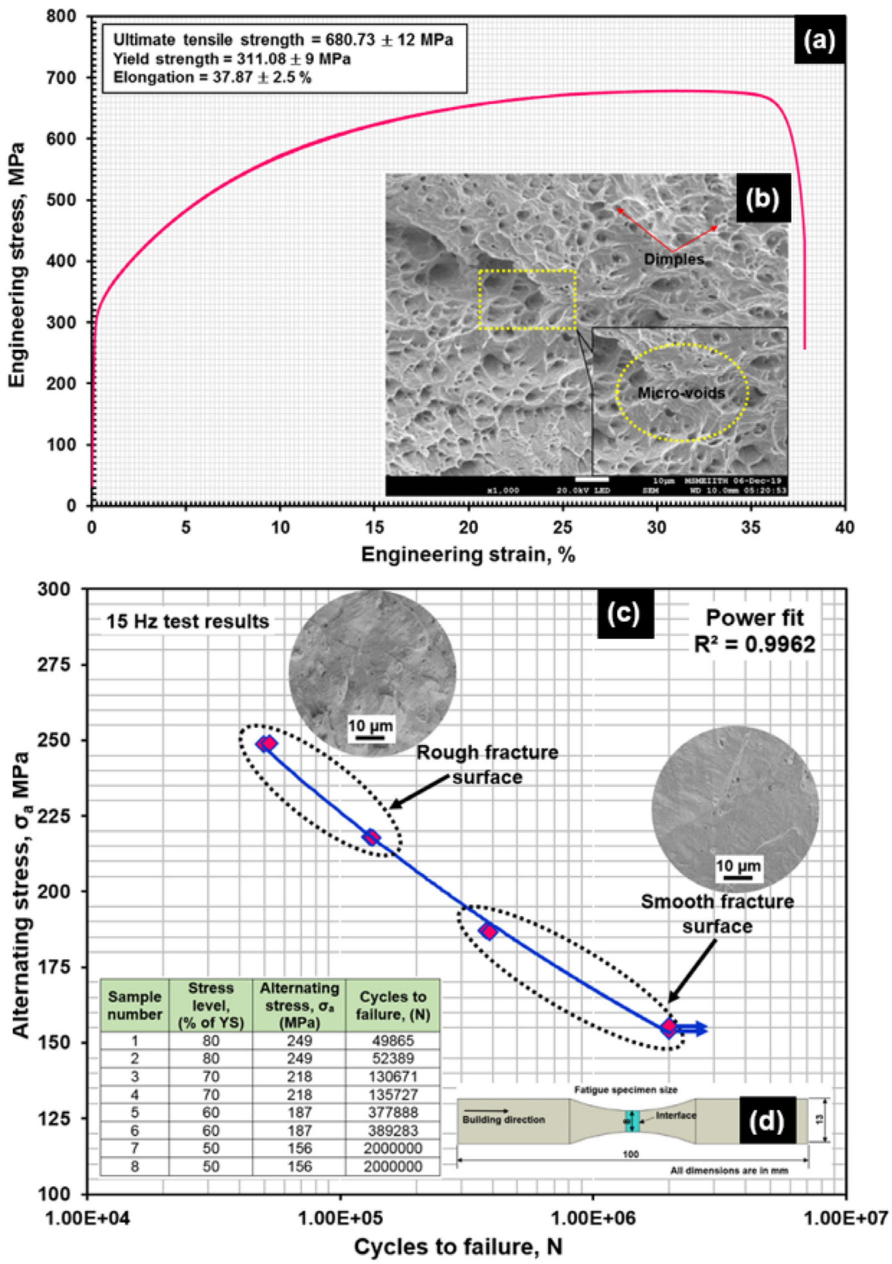

Fig. 2. Monotonic tensile and fatigue test results: (a) Engineering stress vs strain plot, (b) corresponding fractograph, (c) S-N curve and (d) fatigue specimen size.

are presented in Table 1. A single wall of 44 layers were deposited in a to and fro technique to decrease the delineations. The parameters for deposition were: 160 Amps-welding current, 16.4 V- voltage and 250 mm/min-welding speed. The deposition rate was kept constant at 1.18 Kg/h. The multilayered single wall with dimensions of 150 × 120 × 6 mm was machined to 140 × 110 × 4 mm to avail uniform thickness and good surface finish. Samples for microstructural examination were prepared in the as-deposited condition following ASTM E3-11 (2017) along the built direction. Tensile and fatigue samples were prepared using wire-cut EDM following ASTM E8/E8M-16a and ASTM-E466-15 [10] standards, respectively. The fatigue and tensile test specimens were polished to mirror finish. Fully repeated (R = 0.1) stress-controlled fatigue testing was carried out at 80%, 70%, 60% and 50% of yield strength (YS). Two samples were used for each stress percentage. Scanning electron microscope (SEM) was used to examine the fracture morphology of the tensile and fatigue specimens.

3. Results and discussion

The variation in the microstructural features in relation to the built direction of the WAAM processed SS904L/Hastelloy C-276, correspondingly are shown in Fig. 1. Fig. 1a reveals the macrograph of the FGM in as-built condition. Fig. 1(b-d) illustrates the microstructure at SS904L, bi-metallic interface and Hastelloy C-276, respectively. The microstructure was mainly dendritic in the WAAM processed FGM. Fig. 1b shows the presence of equiaxed grains at bottom layers. A cluster of columnar and equiaxed grains were observed at the re-melted layer boundary. Columnar dendrites were observed nucleating from the interface region and transitioning to fully dendritic microstructure as revealed in Fig. 1c. Microstructure at Hastelloy C-276 region highlights the presence of randomly orientated parallel dendrites as depicted in Fig. 1d. In addition, the microstructure was mainly dendritic due to the complex cyclic thermal history (CCTH) experienced during

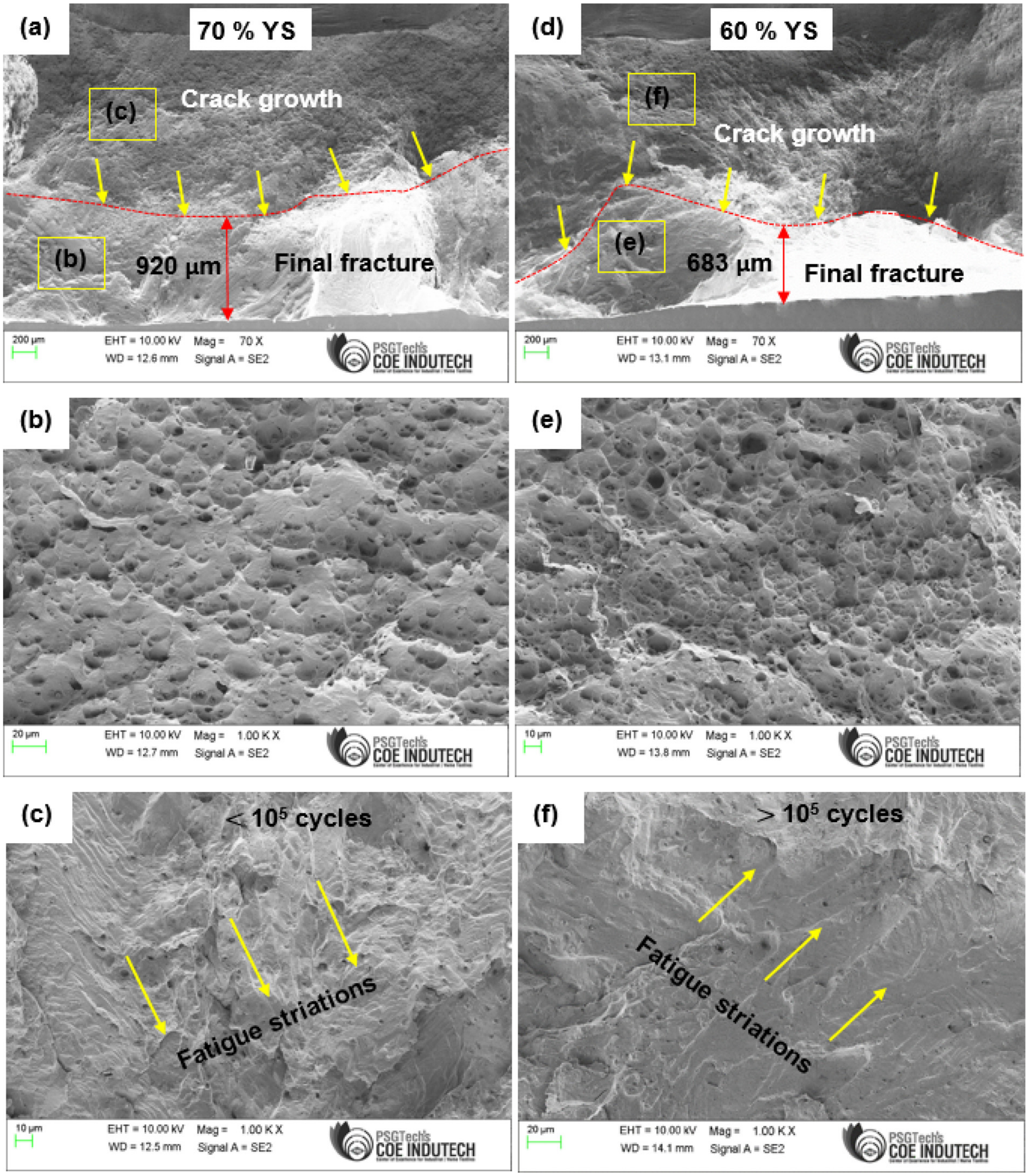

Fig. 3. Representative fracture surfaces of fatigue samples.

the deposition of top layers [11]. Continuous epitaxial growth was observed across the adjacent layers at C-276 region. The bi-metallic interface of the FGM was devoid of solidification cracks as depicted in SEM micrograph (Fig. 1e). Similar kind of microstructures were reported at the interface of AISI 321/Hastelloy C-276 welds [6]. As reported by Chen et al. [12] partial remelting of the previous deposited layer aided the formation of columnar grains, whereby former grains could act as nucleation sites for the subsequent layer solidification. WAAM process accumulates heat as the layers increased, the temperature increases gradually. The temperature gradient of the adjacent deposited layer was lower compared to the former layer, which increased the primary dendrite arms spacing. It is evident from the EDS elemental maps (Fig. 1f) that the dissolution of elements at the interface were uniform and elemental partitioning was absent. EDS line scan examination (Fig. 1g) confirms the absence of intermetallics or secondary phases and highlights the excellent metallurgical bonding at the interface.

The tensile and fatigue test results are presented in Fig. 2. Engineering stress vs strain curve is plotted in Fig. 2a. From the tensile test, the average properties obtained for three samples are presented as an inset column in Fig. 2. The FGM tensile specimens failed in the SS904L region and the tensile strength (680.73 MPa) was higher than the SS904L wrought alloys (490 MPa). The fractured surfaces were characterized with fine dimples and microvoids as shown in Fig. 2b. The FGM samples underwent sufficient plastic deformation before failure and indicates ductile mode of fracture. Fig. 2c illustrates the S-N curve of the FGM samples at various stress levels. The fatigue sample size is shown in Fig. 2d. It is evident from the S-N curve that the sample at same stress level has variation in the number of cycles to failure. This is attributed to the microstructural variations because of CCTH. The right arrow indicates the run-out specimens. In the high cycle fatigue tests, the material having higher ductility shows better fatigue strength [9]. The FGM sample (156 Mpa) showed a decrease in fatigue strength in comparison to the SS904L wrought counterpart (200 MPa) at 2×10^6 cycles [13]. In the present work, the ductility is less compared to the wrought alloys of SS904L & C-276 and this confirms the lower fatigue strength [9]. The R^2 value of the samples tested was 0.9962 and this reveals quality of samples prepared by WAAM.

The Fig. 3 depicts the fractured surfaces of the fatigue specimens and confirms that the FGM specimens were devoid of defects. Fig. 3(a-c) and Fig. 3(d-f) reveals the fracture surfaces of 70% and 60% YS specimens, respectively. For the samples tested < 10^5 cycles, rough surfaces (Fig. 3c) were observed and indicates the plastic deformation from the amount of striations endured and is identical to the previous results [14]. The samples tested > 10^5 cycles revealed a smooth surface indicating lower stress levels (Fig. 3f). The crack growth area increases with decreasing stress levels. The final fracture length showed a decreasing trend from 90% to 60% YS samples. The final rupture surface was observed with voids and dimples and is in line with the previous work [9].

4. Conclusions

Fatigue behaviour of SS904L/Hastelloy C-276 FGM fabricated via WAAM process was evaluated. The SS904L microstructure is composed of equiaxed and columnar dendrites while C-276 shows randomly orientated dendritic grains and is attributed to the CCTH. Continuous epitaxial growth was observed across the adjacent layers at C-276 region. FGM tensile samples fractured with sufficient plastic deformation at SS904L region away from interface and exhibited higher tensile strength than the wrought SS904L alloys. The fatigue strength was 28–35% lower than the SS904L wrought counterparts after sustaining 2×10^6 cycles. Fractographs indicated that surfaces were defect free and specimens fracturing > 10^5 cycles demonstrated smooth surfaces while rough surfaces were observed for < 10^5 cycles.

CRediT authorship contribution statement

A. Rajesh Kannan: Writing - original draft, Data curation. **S. Mohan Kumar:** Invesitigation, Validation.**N. Pravin Kumar:** Data curation, Validation. **N. Siva Shanmugam:** Conceptualization, Methodology, Supervision, Writing – review & editing. **A.S. Vishnu:** Investigation, Formal analysis. **Yasam Palguna:** Investigation, Formal analysis.

Declaration of Competing Interest

The authors declare that they have no known competing financial interests or personal relationships that could have appeared to influence the work reported in this paper.

References

[1] T. DebRoy, H.L. Wei, J.S. Zuback, T. Mukherjee, J.W. Elmer, J.O. Milewski, A.M. Beese, A. Wilson-Heid, A. De, W. Zhang, Prog. Mater Sci. 92 (2018) 112–224.
[2] K. Solberg, S. Guan, S.M.J. Razavi, T. Welo, K.C. Chan, F. Berto, Fatigue Fract. Eng. Mater. Struct. 42 (2019) 2043–2052.
[3] L.L. Wang, J.X. Xue, Q. Wang, Mater. Sci. Eng., A 751 (2019) 183–190.
[4] X. Yang, X. Cui, G. Jin, J. Liu, Y. Chen, Z. Liu, J. Magn. Magn. Mater. 466 (2018) 75–80.
[5] K.D. Ramkumar, S.S. Prabu, N. Arivazhagan, Mater. Res. Express 6 (2019) 086540.
[6] S. Sharma, R.V. Taiwade, H. Vashishtha, J. Mater. Eng. Perform 26 (2017) 1146–1157.
[7] M. Ahsan, A. Tanvir, T. Ross, A. Elsawy, M. Oh, D. Kim, Rapid Prototype J. 26 (2019) 519–530.
[8] Y. Tian, J. Shen, S. Hu, J. Gou, E. Kannatey-Asibu, Sci. Technol. Weld. Joining 25 (2020) 73–80.
[9] L. Carneiro, B. Jalalahmadi, A. Ashtekar, Y. Jiang, Int. J. Fatigue 123 (2019) 22–30.
[10] ASTM Standard E466-15, Standard Practice for Conducting Force Controlled Constant Amplitude Axial Fatigue Tests of Metallic Materials, ASTM International, West Conshohocken, PA, 2003, pp. 1-6. DOI: 10.1520/E0466-15.
[11] A.R. Kannan, N.S. Shanmugam, V. Rajkumar, M. Vishnukumar, Mater. Lett. 270 (2020) 127680.
[12] B. Chen, Y. Su, Z. Xie, C. Tana, J. Feng, Opt. Laser Technol. 123 (2020) 105916.
[13] A. Grigorescu, P.M. Hilgendorff, M. Zimmermann, C.P. Fritzen, H.J. Christ, Fatigue of Materials at Very High Numbers of Loading Cycles, Springer Spektrum (2018) 49–71.
[14] A. Bandyopadhyay, M. Upadhyayula, K.D. Traxel, B. Onuike, Mater. Lett. 255 (2019) 126541.